AGU100 ADVANCING EARTH AND SPACE SCIENCE

Water Resources Research

RESEARCH ARTICLE
10.1029/2018WR023679

Key Points:
- A rapid urban flood inundation model was developed using a novel cellular automata approach and tested against detailed hydrodynamic models
- Our model successfully predicted maximum inundation depth caused by excessive rain and stormwater surcharges within seconds to a few minutes
- Selecting appropriate ranges for the model's parameters is crucial for model performance

Correspondence to:
B. Jamali,
behzad.jamali@outlook.com

Citation:
Jamali, B., Bach, P. M., Cunningham, L., & Deletic, A. (2019). A Cellular Automata fast flood evaluation (CA-ffé) model. *Water Resources Research*, *55*, 4936–4953. https://doi.org/10.1029/2018WR023679

Received 15 JUL 2018
Accepted 22 MAY 2019
Published online 21 JUN 2019

A Cellular Automata Fast Flood Evaluation (CA-ffé) Model

Behzad Jamali[1,2], Peter M. Bach[2,3,4], Luke Cunningham[5], and Ana Deletic[1]

[1]Water Research Centre, School of Civil and Environmental Engineering, University of New South Wales, Sydney, New South Wales, Australia, [2]Monash Infrastructure Research Institute, Department of Civil Engineering, Monash University, Clayton, Victoria, Australia, [3]Swiss Federal Institute of Aquatic Science and Technology (Eawag), Dübendorf, Switzerland, [4]Institute of Environmental Engineering, ETH Zürich, Zürich, Switzerland, [5]Water Technology Pty Ltd, Notting Hill, Victoria, Australia

Abstract The simulation speed of two-dimensional hydrodynamic flood models is a limiting factor when catchments are large, a considerable number of simulations is required (e.g., exploratory modeling, Monte-Carlo flood simulations, or predicting probabilistic flood maps), or when there is a need for real-time flood emergency management. Rapid Flood Models (RFMs) that rely only on topographic depressions and the water balance equation have been successfully implemented to predict maximum urban flood inundation depths within seconds to a few minutes. However, the preprocessing step (identification of depressions and their attributes) and the postprocessing step (marking up possible flow paths of flood water in between flooded depressions) of RFMs is time consuming. In this study, we developed a new fast flood inundation model based on the cellular automata (CA) approach. The new model does not require the preprocessing and postprocessing steps of RFMs and therefore can provide more simulation speed. The performance of our new model, referred to as Cellular Automata fast flood evaluation (CA-ffé), was compared to two well-known hydrodynamic flood models (HEC-RAS and TUFLOW) in 20 simulation experiments conducted in five different urban subcatchments. CA-ffé predicted maximum inundation depth with reasonable accuracy in a matter of seconds to a few minutes for a single rainfall event simulation. The CA-ffé model performed exceptionally well in areas with low-lying depressions. However, in areas where floodwaters had higher momentum and velocity, the model usually was not able to estimate inundation depths calculated by HEC-RAS or TUFLOW. CA-ffé's key drawback is also its inability to represent the temporal evolution of flooding and flow velocities. Nevertheless, its ability to provide spatial flood extents and depths in a fraction of the time compared to its hydrodynamic counterparts is a significant advancement toward exploratory approaches for water systems planning, model-based predictive control, and real-time flood management.

1. Introduction

The application of 2-D hydraulic modeling packages for urban flood inundation prediction has become widespread due to greater availability of high resolution digital terrain models and high-performance computational resources (S. Néelz, 2009). Selection of an appropriate flood model usually depends on the context and purpose of the study, required and available input data, desired output variables, their spatial and temporal resolution, level of accuracy, and computational demands (Teng et al., 2017). Flood risk analysis in urban areas usually involves accurate prediction of flow velocities and depths. As such, detailed hydrodynamic models (i.e., models that solve the full shallow water equations [SWEs]) are often used. Due to their long simulation run time, such detailed models are neither economical nor even feasible when myriad flood simulations are required such as in cases investigating spatial and temporal rainfall variability (Simões et al., 2015) or combining the impact of fluvial and pluvial floods in probabilistic-based flood hazard analysis (Apel et al., 2016). Additionally, these models struggle to simulate urban flood inundations in large catchments (e.g., over 20 km^2). The emergence of parallel computing and graphics processing units have improved the speed of detailed hydrodynamic models. However, these models are inherently characterized as a series of sequential computations and, therefore, not always able to take full advantage of parallel processing capabilities (Guidolin et al., 2016). Furthermore, running a parallel version of these models demands higher computational resources (e.g., a single desktop computer is not enough). Some models reduce the complexity of the SWEs by neglecting or approximating less important terms (e.g., Urban Inundation Model by Chen et al., 2007, and LISFLOOD-FP by Bates & de Roo, 2000). A combination of these methods might also be

implemented. For example, to enable national and global scale flood simulations, the computational speed of solving a simplified form of SWEs (Bates et al., 2010) was further improved through algorithm parallelization (Sampson et al., 2015; Wing et al., 2017). Despite the simplifications made in these models, these equations remain complex and are computationally expensive to implement (Guidolin et al., 2016). There has recently been a growing number of flood models that do not attempt to solve SWEs but use very different fundamental approaches. According to their level of complexity, we group these urban flood inundation models into two categories: (i) models based on cellular automata (CA) and (ii) models based on topographic depressions.

1.1. Models Based on CA

These models discretize the flood domain into a regular grid of cells, each having a number of states. Spatiotemporal evolution of flooding is translated into a set of general transition rules that update the states of each cell according to the states of their neighbor cells and its own state from the previous time step. These models use the Manning equation or alternative empirical relationship for uniform flow, such as the Chezy or weir equation to calculate intercellular flux rates in each time step (Dottori & Todini, 2011). Ghimire et al. (2013) applied a simple method that ranked neighbor cells according to their water level. Water flow was driven mainly by the hydraulic gradient between cells and limited to the transferrable volume calculated by the Manning's and critical flow equations. Their model was up to 30 times faster than the Urban Inundation Model that uses a simplified form of the Saint-Venant equations (Albert S. Chen et al., 2012). Guidolin et al. (2016) further simplified this method in their Weighted Cellular Automata 2-D (WCA2D) model. WCA2D calculates the ratio of water transfer from the central cell to the downstream neighbor cells (intercellular volume) using a weight-based approach and limits them by applying the Manning's formula and the critical flow equation only once per central cell. Demonstrations show that WCA2D can run up to eight times faster than the commercial software InfoWorks ICM 3.0 (Innovyze, 2012) in a real world case study (Guidolin et al., 2016). CA-based models are diffusive-like models which require very small time steps when the cell sizes are small. To ensure numerical stability, modeling time step should be reduced quadratically with the decrease in the cell sizes. Therefore, their computational speedup decreases for simulating urban flooding with high-resolution model grids (e.g., 1 m or smaller). Despite significant improvement in the computational efficiency of CA-based models in recent years, their simulation times are still significantly higher than *models based on topographic depressions*, which are designed to run within seconds.

1.2. Models Based on Topographic Depressions

These models consider topography and the continuity equation to predict inundation areas and, therefore, have run times in orders of magnitude shorter than detailed hydrodynamic models (Teng et al., 2017). Hereon, we refer to these as Rapid Flood Models (RFMs). RFMs have lower level of complexities and higher simulation speeds compared to CA-based models. Simulation speedup is achieved mainly by disregarding the temporal evolution of flooding (e.g., Gouldby et al., 2008; Krupka, 2009; Lhomme et al., 2008). Unlike CA-based models, which use a regular grid of cells, RFMs divide the flood calculation domain into elementary areas called impact zones (IZs), which represent natural depressions in the ground (Lhomme et al., 2008). The size of IZs are significantly larger than grid cells in CA-based models which makes RFMs computationally more efficient. A number of studies have tried to improve these models by better representing the mechanisms of flow exchange between storage zones and by introducing temporal dynamics of flooding (Bernini & Franchini, 2013; CH2M, 2013; Liu & Pender, 2010). Despite the absence of temporal dynamics, RFMs have been successful in assessing flood damage cost in urban areas among other potential applications.

Figure 1a shows the three steps of flood inundation modeling generally used in RFMs: (i) preprocessing step for delineating IZs and their attributes (e.g., area-volume relationship, list of neighboring IZs, and communication points and levels); (ii) flood spreading step for computing water levels in each IZ; and (iii) postprocessing step for producing flood inundation maps. Figure 1b shows the flood spreading step for a simple case with one inflow point (Lhomme et al., 2008):

1. Overtopped volume is passed to the IZ adjacent to the breach location (IZ B).
2. IZ B fills up to its lowest communication level (CL). The communication level of an IZ determines the level at which the excess volume spills toward neighboring IZs. (IZ C in this case).
3. The water level in IZ C is set to the first CL, as shown in Figure 1, IZ C has the same water level as IZ B.

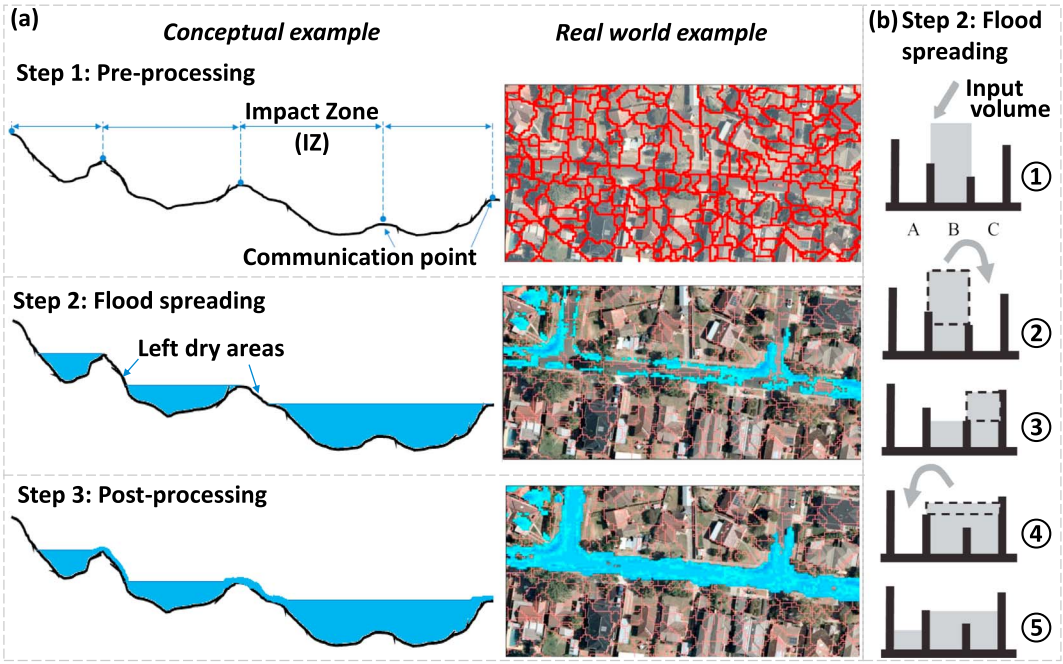

Figure 1. The three steps of Rapid Flood Models: preprocessing (for delineating impact zones and their attributes), flood spreading, and postprocessing for filling up left dry areas (a); and the spilling/merging process of flood spreading step (b) adapted from Lhomme et al. (2008).

4. IZs B and C are merged, the water level is increased to the first CL, and the excess volume is spilled toward IZ A.
5. The water volume is lower than the capacity of IZ. Hence, the process stops.

Once the water levels in each impact zone is estimated, the postprocessing step converts these levels into flood depth maps. One of the limitations of rapid inundation models is that their simple filling/spilling algorithm tends to leave isolated flooded areas in between IZs (which are natural flow paths) as dry areas (Jamali et al., 2018). Some RFMs such as the ISIS FAST model (CH2M, 2013) have an additional processing step that uses a version of a rolling ball algorithm to find the path water may have taken between isolated flooded areas (Figure 1a).

In our recent study (Jamali et al., 2018) we developed an RFM model, referred to as RUFIDAM (Rapid Flood Inundation and Damage Assessment Model). Our results showed that the preprocessing step of RUFIDAM takes 2 to 10 min for catchments with sizes between 0.8 and 10 km^2 and using a 1-m-resolution digital elevation model (DEM). A similar amount of time was required to finish the flood spreading and postprocessing steps (RUFIDAM did not include the process for marking up "left-dry" flow path areas. In general, their model was 40 to 550 times faster than the MIKE FLOOD hydrodynamic model case studies. The preprocessing step of RUFIDAM was not only time-consuming, but it also required the modeler to find the appropriate parameter set (such as minimum depth and area for IZs) to get the desired accuracy in their results. In most cases, preprocessing is only required to be carried out once. However, this step should be repeated in studies that include simulating land use change scenarios (e.g., due to urban growth) and flood simulations (e.g., Löwe et al., 2017). The process of marking up left-dry areas will also add to the simulation time. Therefore, elimination of the preprocessing and postprocessing steps will increase the simulation time, if flood spreading takes equally long.

In this study, we developed a fast urban flood inundation model, named the Cellular Automata fast flood evaluation (CA-ffé) model, which can simulate flood inundation in urban areas due to point inflows (e.g., surcharges from drainage network manholes or channels) and also from rainfall applied directly to the surface area (also known as the "rainfall on the grid or direct rainfall" approach, EA, 2012). Using an innovative simplified flood spreading algorithm based on the CA approach, CA-ffé provides a method that does not require the time-consuming preprocessing step for identification of IZs and their attributes, and

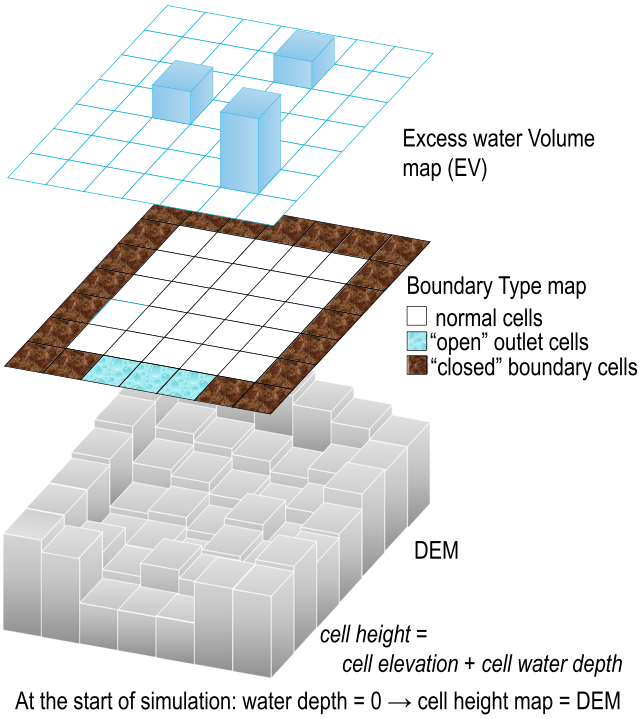

Figure 2. Cellular automata lattice, type of cells and neighborhood in the Cellular Automata fast flood evaluation model.

postprocessing step for identifying and marking-up potential flow paths in between flooded IZs. Similar to RFMs, our model only relies on topography and the continuity equation and only predicts the final flood extent and depth. Unlike the CA-based flood models that use the Manning equation (or similar empirical relationships) to spread water between cells (e.g., Ghimire et al., 2013; Guidolin et al., 2016), CA-ffé implements a novel algorithm that does not have a modeling time step. Therefore, when higher grid resolutions are used, its computational performance does not decrease as much as diffusive-like CA-based models. CA-ffé uses simple rules to spread water among cells and can simulate a typical urban flood event at neighborhood scales (e.g., up to 25 km^2 and 1-m-grid resolution) within seconds to a few minutes. CA-ffé does not model flow in channels and rivers. However, it can be coupled to one-dimensional (1-D) drainage network or river/channel models to simulate the inundation caused by surcharged/overtopped flows from manholes or rivers. We successfully tested CA-ffé against the TUFLOW (WBM, B, 2016) and HEC-RAS (Hydrologic Engineering Center, 2016) – two well-known and widely used hydrodynamic models – by applying it to four urban catchments of different characteristics.

2. Materials and Methods

2.1. CA-ffé Model Structure

The CA-ffé model combines the most attractive attributes of CA-based flood models and RFMs to predict urban flood inundation. In this section, we briefly explain the theoretical background of the two approaches.

CA-ffé uses a regular grid of cells instead of IZs. Therefore, it does not require the preprocessing step to identify IZs. Furthermore, using regular grids in our CA-based algorithm, we addressed the problem of finding possible flow path areas in RFMs. As regular grid cells, however, represent much smaller IZs in RFMs, this would increase the number of calculations and simulation time. Our CA-based model algorithm eliminates the merging process in the algorithm that Lhomme et al. (2008) introduced (outlined earlier in Step 4). The merging process happens when two (or more) adjacent wet IZs have the same water levels. In this condition, they form one larger IZ and then attributes of the new IZ and (i.e., storage-area relationship and list of new neighbors) are updated. This is computationally expensive and can significantly increase model runtime if the number of IZs is high. Our CA-based model is developed in the Python 2.7.12 (http://www.python.org) using the Geospatial Data Abstraction Library (GDAL Development Team, 2018) and does not use parallel or graphics processing unit computations.

2.1.1. Definition of Model Input Grids

CA-ffé takes four grid maps as input: DEM, cell height, boundary type, and cell Excess water Volume (EV; see Figure 2). These maps have the same number of rows, columns, and georeferencing. CA-ffé uses a DEM grid as the lattice of CA cells. Although we implement a square grid DEM for its simplicity and broader application (Shao et al., 2015), the algorithm can be adapted to work with other types of grids such as hexagonal (de Sousa et al., 2017) or irregular triangular grids. The grid resolution of CA-ffé is automatically set to the input DEM's resolution. If a different model resolution is required, the DEM is resampled first to the required resolution (using Geospatial Data Abstraction Library functions in Python) and then used in CA-ffé. Sensitive high or low points (e.g., creek centerline or levee walls), can be predefined using a line or polygon map. DEM resampling can be conditioned to apply maximum and minimum flags to the cells for these areas.

The cell height map represents the sum of cell ground elevation (from the DEM map) and water depth. At the start of the simulation, if there is no flood water on the surface, cell height is equal to the ground elevation since the water depth of all cells is equal to 0. Alternatively, the simulation can start with predefined nonzero water depths as initial boundary condition (e.g., when there is preexisting inundation or defined downstream water levels).

The boundary type map indicates how border cells in the CA lattice are treated. Border cells can be either "closed" boundary cells which no water can flow beyond them, or "open" boundary cells that represent the outlets of the study area and will absorb any water flowing into them (Shao et al., 2015). All water that enters open outlet cells will be lost from the calculations and recorded as the volume of outflow from the study area. By default, the ground elevation of closed boundary cells in the DEM map is increased by 100 m to ensure that water will not exit from these cells. Closed boundary cells can also be used to represent structural barriers to flooding such as dikes. In this case, users can modify the increase in elevation of closed boundary cells. When the user is not familiar with the outflow locations of the study area, it is recommended to run preliminary flood simulations to identify potential outflow areas and use this information to set the boundary type of border cells.

The EV map represents the flood water volume overtopped on a cell. Total EV is the sum of flood volume that should be spread by the model. This can be generated by excess rainfall on a cell and point source discharge volume (e.g., underground drainage network manholes or breached/overtopped point(s) in a river/canal). At this stage, we do not simulate or account for hydrological losses (e.g., interception and infiltration) in the model. Rainfall can be uniformly distributed over the catchment or spatially variable depending on the type of storm simulated.

2.1.2. Application of Transition Rules

Similar to the CA models in Bennett et al. (2013) and Ghimire et al. (2013), we use the von-Neumann (VN) neighborhood, meaning that water can flow from the central cell in four cardinal directions (north, south, east, and west). At each simulation iteration each cell in the calculation domain will be visited and one of the following transition rules (Figure 3) will be applied:

Rule 0—Do Nothing: if the central cell has no EV. The simulation ends when there is no excess volume left to be spread (i.e., there is no cell with EV > 0).

***Rule 1—Ponding*:** if the central cell height is lower than its neighbors' cell height, increase water level up to the level of the lowest neighbor height and deduct this volume from the cell's EV. If the increased volume is higher than the cell's EV, only raise water level to match the cell's EV.

***Rule 2—Spreading*:** if the central cell height is equal to its neighbors' cell height, the central cell's EV will be equally shared among the five cells. The cell heights do not change in this condition since these five neighboring cells might have neighbors with lower levels and the EV will flow into them in the next iteration.

***Rule 3—Increasing Level*:** if the central cell's height is equal to the height of one, two, or three neighbors and less than the height of the others, the central cell height will increase by a constant value selected by the user, termed "increment constant." The equivalent volume will be deducted from the central cell's EV. The remaining EV will be equally divided between neighboring cells with the same level. Rule 2 and 3 represents the filling process of a topographic depression that is formed by a group of cells. Rule 2 spreads EV among cells, and Rule 3 raises the water level in depression by an increment constant when water hits the borders of the depression. It should be noted that the increment constant is the water that is trapped in a depression and will not be redistributed again. Therefore, selecting a large increment constant value could result in poor model performance. On the other hand, a small increment constant will increase the number of iterations required to fill up depressions and increase the simulation time.

Rule 4—Partitioning: applies when none of the above rules are applicable. In this rule, the central cell's height will be greater than the cell height of at least one neighbor and therefore all the EV in the central cell should eventually drain to the "downstream" neighbor(s).

The central cell in Rule 4 acts as a flow path cell, meaning that all the EV will be transferred to the downstream neighbor(s). In real world conditions, the depth at which water flows downstream depends on several factors such as the flow rate, friction coefficient, and slope. In Rule 4, water depth in the central cell will

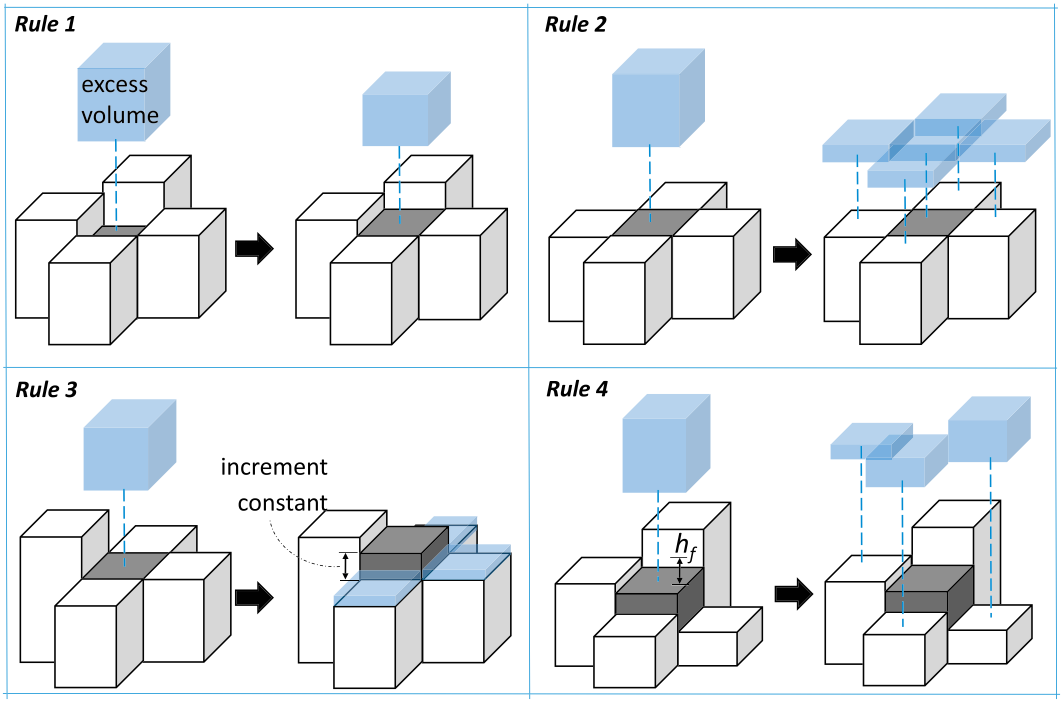

Figure 3. Illustration of Cellular Automata fast flood evaluation's transition rules. A different example is used for each rule to show their application (dark = central cell; blue dashed lines = which cell the excess volume belongs to).

temporarily increase to overcome the friction head loss. This depth is referred to as h_f and is a function of EV in the central cell:

$$h_f = a \times EV^b \tag{1}$$

where a and b are constant coefficients that are estimated independently during model calibration using the performance indicators described in section 2.2.2 which measure accuracy of the model in predicting both flood extent and depths. The power type equation for h_f parameter was inspired by the rating curves in hydrology, which relate river stage to flow rates. Our preliminary analysis showed that power equation performs better than linear and exponential forms of the equation.

A downstream neighbor is defined as a cell lower than the central cell plus h_f. Downstream neighbors will receive EV from the central cell according to a weighting system similar to Guidolin et al. (2016) as shown in the following equations:

$$d_i = \max\left(0, H_0 + h_f - H_i\right) \tag{2}$$

$$w_i = \frac{d_i}{\sum_{i=1}^{4} d_i} \tag{3}$$

$$EV_i += w_i \times EV_0 \tag{4}$$

H_0 and H_i denote the height of central 0 and neighbor cell i, respectively. The excess volume in the central cell EV_0 is divided between downstream cells based on proportional weightings w_i (cells that are not downstream neighbors of central cell 0 will have a w_i of 0).

Rules 1, 2, and 3 together emulate the filling process of a topographic depression. Rule 4 on the other hand maps the flow path by determining the potential path water can take from one cell to another. Therefore, CA-ffe does not require an additional postprocessing step used in RFMs to mark up left dry areas in between flooded depressions.

It should be noted that an iteration in our model should be considered as a "time step" in hydrodynamic flood models. When Rule 1 is applied, a CA-ffé model iteration means that the central cell located in depression will be filled, regardless of how long it is going to take to do so. Similarly, when Rule 4 is applied, an iteration means that all the excess volume in the central cell will be transferred to the downstream neighbors, regardless of how long it would take to do so. Therefore, the model internally does not keep track of time.

At the end of the simulation (i.e., when there is no excess volume left to spread), CA-ffé produces maps of final and maximum flood depths. The final flood map shows the state of flooding where all the water is drained from the flow path areas and ponded in topographic depressions. The maximum flood map shows the highest water depth occurring in a cell during model simulation. Therefore, it includes flood depth information in both depressions and flow path areas. Maximum flood inundation maps are widely used for assessing flood damage costs (e.g., Jamali et al., 2018; Löwe et al., 2017).

2.2. CA-ffé Model Performance

2.2.1. Case Studies

We tested CA-ffé in a range of simulation experiments using five different case studies (Table 1): four urban subcatchments located in the Mordialloc Creek and Elster Creek Catchments, Melbourne (Australia), and one small urban area in the UK, used in the Environment Agency's (EA) benchmarking Test 8a for 2-D flood models (the EA benchmarking tests (Néelz & Pender, 2013) were applied to a number of 2-D hydraulic modeling tools to investigate their capabilities in different conditions). Each case study was compared with a hydrodynamic model set up for the same area using either HEC-RAS (Hydrologic Engineering Center, 2016) or TUFLOW (WBM, B, 2016; see Table 1 for details). These five case studies represent different urban flood conditions and therefore enable robust testing of the CA-ffé model.

The four subcatchments in Melbourne were historically affected by pluvial flooding as a result of surcharges from the pipe network. Therefore, the main source of flooding in these case studies is surcharge from the stormwater system, coming from stormwater inlets or manholes as point sources. Surcharge flows were simulated using the SWMM (Rossman, 2015) 1-D drainage network model for a number of design storm events with different return periods. Subcatchments 1, 2, and 4 were tested using the results of a 100-year storm event SWMM simulation. To simplify the setup process of the HEC-RAS and TUFLOW models, inflow points with a small surcharge volume were grouped with points that had a larger surcharge volume. Total surcharge volume in Subcatchments 1 and 2 were around 8,000, 24,000, respectively. In Subcatchment 3 we tested CA-ffé for different flood magnitudes by running SWMM for 10-, 50-, and 100-year design storm events, which produced a total surcharge of 10,000, 28,000, and 50,000 m^3, respectively. It should be noted that CA-ffé has no limitation on the number of surcharge points and volumes as it is automatically coupled to the SWMM model. Therefore, in the real-world cases there was no need for grouping the surcharging nodes.

In the fifth case study, CA-ffé was tested for Test 8a, where flooding originated from two sources: runoff generated by applying a uniformly distributed (effective) rainfall to the modeled area and an inflow point (as a surcharging node in drainage network). Table 1 shows the number of surcharge points and total flood volume spread in each subcatchment. In all the case studies there was no river or channel, and the interaction of surface area with drainage system was not included. It should be noted that CA-ffé can be coupled to 1-D river/channel or stormwater drainage models to simulate the inundation caused by any source of flooding. Not including 1-D models eliminated potential discrepancies that could have been caused by differences in 1-D model predictions. We refer the reader to Jamali et al. (2018) for a discussion on coupling RFMs with 1-D drainage network models. Similar to the previous studies (Guidolin et al., 2016) and following the EA Test 8a setups (Néelz & Pender, 2013), it was assumed that the catchment area was fully impervious, indicating a fully saturated impervious areas in urban areas after a large storm event. The reason for this assumption is to limit the focus of the test on the flood spreading algorithms on the surface.

Subcatchments 1, 2, and 3 were compared to the results obtained from the HEC-RAS version 5.0.6 (Hydrologic Engineering Center, 2016). This model utilizes an implicit finite volume algorithm to solve full Saint Venant Equations. The results of Subcatchment 4 were compared to the results of an existing TUFLOW model setup for the study area. Different versions of TUFLOW are equipped with either finite

Table 1
List of the Case Studies and Simulation Experiment Details Used for Model Validation

Case study	Characteristics	Manning's n ($m^{-1/3}s$)	Flooding source, magnitude, and inflow duration	Grid size, simulation time step, and simulation length	Validation	
					HEC-RAS	TUFLOW
S1 Mordialloc Creek, Melbourne	size: 30 ha elevation: 39.7–47.1 m slope: 2.3%	0.03, 0.05 and 0.07	1 stormwater surcharge total volume:8,000 m^3 (100-year storm event) ~70 min	1 m; 0.5 s until t = 4 hr	✓	
S2 Mordialloc Creek, Melbourne	size: 1.4 km^2 elevation: 41.3–53.7 m slope: 4.3%	0.03, 0.05 and 0.07	8 stormwater surcharges total volume:24,000 m^3 (100-year storm event) ~70 min	1 m; 0.5 s until t = 4 hr	✓	
S3 Elster Creek, Melbourne	size: 2.4 km^2 elevation: 1.5–25.6 m slope: 4.8%	0.03, 0.05 and 0.07	20 stormwater surcharges 3 storm events with total volumes: 10,000 m^3 (10 years) 28,000 m^3 (50 years) 50,000 m^3 (100 years) ~70 min	1 m; 0.5 s, 2 m; 1 s, 4 m; 2 s, 5 m; 2 s, until t = 4 hr	✓	
S4 Elster Creek, Melbourne	size:14.4 km^2 elevation: 20.6–58 m slope: 4.1%	0.05	30 stormwater surcharges total volume: 111,500 m^3 (100-year storm event), ~70 min	1 m; 0.5 s, 2 m; 1 s, 4 m; 2 s, 5 m; 2 s, until t = 8 hr		✓
Test 8a from the EA Benchmark Study[a]	size: 0.4 km^2 elevation: 21–37.6 m slope: 4.3%	0.02 for road; 0.05 for other surfaces	direct rainfall (~27 mm), 4 min/and 1 stormwater sewer surcharge (~4,300 m^3), 30 min	0.5 m; 0.2 s until t = 7 hr	✓	✓

[a]Néelz and Pender (2013).

difference or finite volume schemes. The EA benchmarking test compared CA-ffé with both HEC-RAS (5.0.6) and TUFLOW (version 2018-03-AA) simulation results.

All catchments were initially tested for the highest-resolution grid that was available; 1 m for Subcatchments 1 to 3 and 0.5 m for Test 8a. In order to check CA-ffé's performance for different surface roughness conditions, Subcatchments 1, 2, and 3 had different Manning's n values (0.03, 0.05, and 0.07 $m^{-1/3}$ s, respectively) that were uniformly applied to the modeled area. Subcatchment 4 had a Manning's roughness value of 0.05 $m^{-1/3}s$. For the EA Test 8a we applied a value of 0.02 $m^{-1/3}s$ for road pavements and 0.05 $m^{-1/3}s$ for other surface areas (see Table 1).

2.2.2. Performance Indicators

We compared the maximum flood depth maps of CA-ffé with the similar results produced by HEC-RAS and TUFLOW. For this purpose, we used five common model performance indicators explained in Table 2 (Bennett et al., 2013): (i) hit rate (HR), (ii) false alarm rate (FAR), (iii) critical success index (CSI), (iv) root-mean-square error (RMSE), and (v) Nash-Sutcliffe efficiency (NSE). In calculating each of these indicators, we defined "inundated" cells as those that have a water depth greater than 5 cm. This threshold is commonly used to define areas as flooded because inundations larger than 5 cm can cause damage to basements, roads and railways (Kaspersen & Halsnæs, 2017). HR represents the number of cells that are predicted as inundated in both the CA-ffé and the hydrodynamic model. It indicates what fraction of inundated cells in the hydrodynamic model is predicted as inundated in the CA-ffé model. FAR represents the number of cells that are inundated in CA-ffé but unaffected (water depth < 5 cm) in the hydrodynamic model. FAR indicates what fraction of the predicted inundated cells by CA-ffé did not occur in the hydrodynamic model. HR indicator ignores false alarms, and FAR ignores misses. The CSI is a balanced score because it is sensitive to both misses and false alarms. It measures the fraction of cells cases that were correctly predicted (Bennett et al., 2013).

These indicators compare the maximum inundated area predicted by the two models while considering the depth threshold. However, they do not measure the accuracy of the model in predicting the flood depth. The RMSE and NSE indicators take into account deviations in the predicted depths. In calculating RMSE

Table 2
Performance Indicators Used for Comparing CA-ffé Against HEC-RAS and TUFLOW Models

Performance index	Formula	Range	Optimal score
HR (%)	$HR = \frac{Hits}{Hits+Misses} \times 100$	0–100%	100%
FAR (%)	$FAR = \frac{False\ alarms}{Hits+False\ alarms} \times 100$	0–100%	0%
CSI (%)	$CSI = \frac{Hits}{Hits+Misses+False\ alarms} \times 100$	0–100%	100%
RMSE (m)	$RMSE = \sqrt{\frac{\sum_{i=1}^{n}\left(Y_i^C - Y_i^T\right)^2}{n}}$	0–∞	0
NSE	$NSE = 1 - \left[\frac{\sum_{i=1}^{n}\left(Y_i^C - Y_i^T\right)^2}{\sum_{i=1}^{n}\left(Y_i^T - Y_{mean}^T\right)^2}\right]$	−∞ to 1	1

Note. CA-ffé = Cellular Automata fast flood evaluation; HR = hit rate; FAR = false alarm rate; CSI = critical success index; RMSE = root-mean-square error; NSE = and Nash-Sutcliffe efficiency.

and NSE, we considered those cells that are inundated in either CA-ffé or hydrodynamic or are inundated in both models.

2.2.3. Sensitivity of CA-ffé to the Key Model Parameters and Grid Size

We conducted a series of sensitivity analyses to investigate how CA-ffé's predictions varied based on the two model parameters: the increment constant parameter (Rule 3 in section 2.1) and the temporary depth of water (h_f functions in Rule 4). The work was undertaken on Subcatchments 1, 2, and 3, for the 100-year storm event and for three Manning's n values of 0.03, 0.05, and 0.07 $m^{-1/3}s$ (nine sensitivity tests in total; see Table 1). This was also considered as a calibration procedure to identify the parameter range for which the best performance indicators (Table 2) were achieved.

For each subcatchment we conducted 4,000 CA-ffé simulations with various parameter sets created using a grid-search approach by 200 values of increment constants ranging between 1×10^{-5} to 1 m and 20 different h_f functions (see Figure 4). Prior to the sensitivity analysis, we conducted preliminary simulations in Subcatchments 1, 2, and 3 to help selecting the appropriate ranges for the coefficients a and b (equation (1)) and for the increment constant parameter. Our preliminary results showed that CA-ffé performed equally well when b was within the range of 0.05 to 0.3. This was mainly because the changing the value of b does not significantly change the shape of h_f function curves. However, CA-ffé's performance was very sensitive to the coefficient a. Therefore, for the purpose of sensitivity analysis, the 20 different h_f functions were created by ranging a between 0.01 to 0.2 and selecting a constant value of 0.25 for coefficient b.

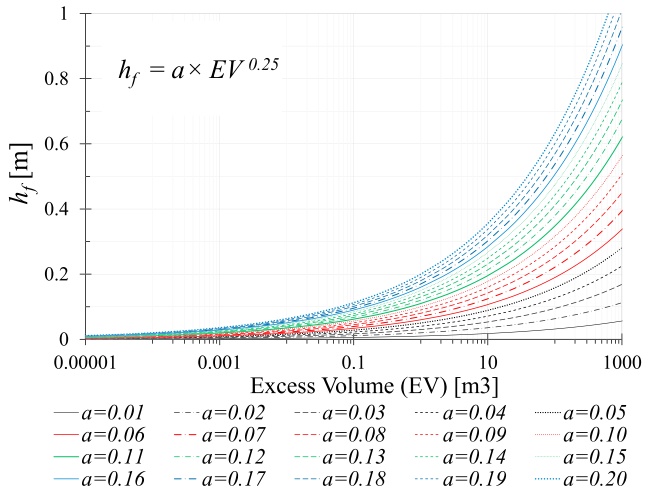

Figure 4. h_f functions used in the sensitivity analysis of the Cellular Automata fast flood evaluation model. These functions were created using equation (1) with b = 0. 25 and 20 values of a = 0.01, 0.02, ... , 0.2.

The maximum flood depth maps predicted in each CA-ffé simulation was compared to the maximum inundation depth predicted by HEC-RAS using the five performance indicators. We also produced two sensitivity plots using parameter sets that produced CSI and NSE indicators above a certain threshold. These sensitivity plots indicate model parameter range for which the model performance reaches to a certain threshold. The threshold for each sensitivity analysis test was selected to be 95% of maximum estimated CSI or NSE values for that test case.

We also investigated the sensitivity of CA-ffé's performance to the DEM grid resolution. For this purpose, eight CA-ffé simulations were carried out by varying the DEM grid resolution in Subcatchments 3 and 4. Using the ArcGIS Resample toolset (ESRI, 2012), we obtained three DEMs of 2-, 4-, and 5-m resolutions from a 1-m-resolution lidar grid. We used the 100-year event surcharge volume for these CA-ffé simulations and compared the results to the hydrodynamic models with the same grid resolution.

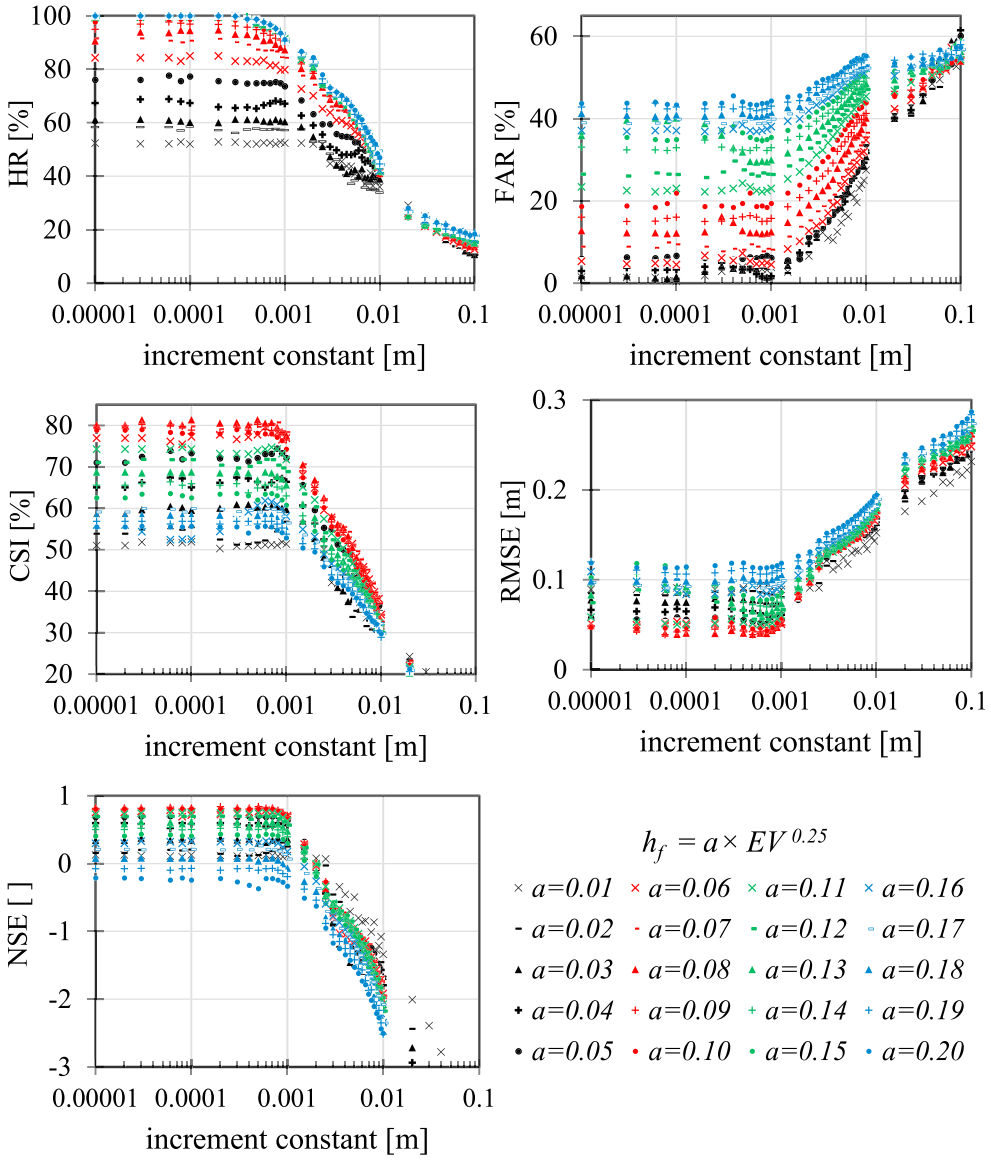

Figure 5. Sensitivity analysis of key model parameters: increment constant (1×10^{-5} to 0.1 m) and 20 h_f functions created using equation (1) with $b = 0.25$ and $a = 0.01, 0.02, \ldots, 0.2$. Results belong to Subcatchment 1 (100-year event with 1-m-resolution grid) and are created using the five performance indicators: hit rate (HR), false alarm rate (FAR), critical success index (CSI), root-mean-square error (RMSE) and Nash-Sutcliffe efficiency (NSE).

3. Result and Discussion

3.1. Sensitivity Analysis of the CA-ffé Model Parameters

We first discuss the results of our sensitivity analysis on key model parameters as these provided the calibrated values that we used throughout all remaining case studies. Figure 5 shows the calculated performance indicators used in the sensitivity analysis conducted in Subcatchment 1 for Manning's $n = 0.03$ $m^{-1/3}s$. As shown in this figure, CA-ffé's performance is sensitive to the selected increment constant and h_f function. As explained in Rule 3 (section 2.1.2), it is expected that selecting a smaller increment constant would lead to better model performance. Figure 5 shows that decreasing the increment constant from 1 m to around 0.001 m improves the performance indicators in all h_f functions. For increment constants smaller than 0.001 m, model performance did not improve despite small fluctuations. The sensitivity analysis results from Subcatchments 2 and 3 and for other Manning's n values showed the same behavior. This indicates that

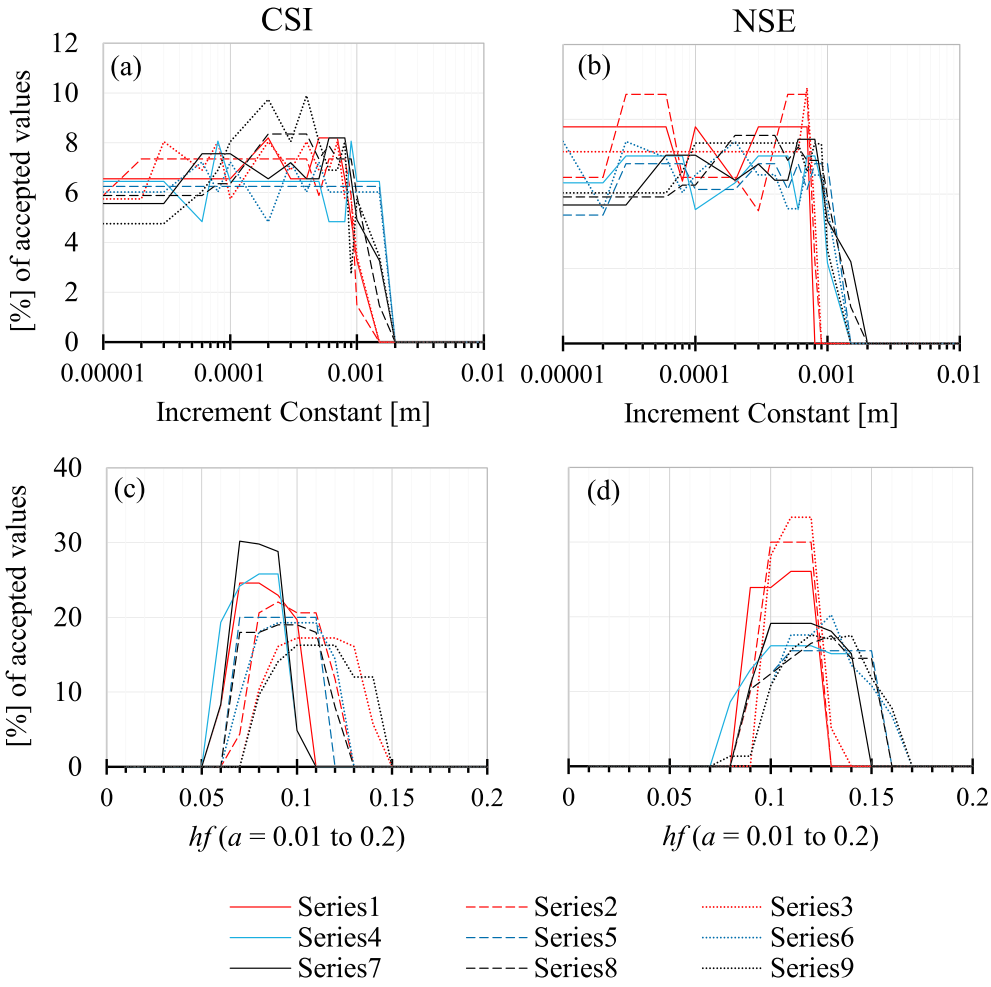

Figure 6. Sensitivity analysis plots of Cellular Automata fast flood evaluation model parameters: increment constant (a and b) and h_f function (c and d) using the CSI (a and c) and NSE (b and d) performance indicators in Subcatchments 1, 2, and 3 and for Manning's n of 0.03, 0.05, and 0.07 $m^{-1/3}s$. CSI = critical success index; NSE = Nash-Sutcliffe efficiency.

selecting increment constant values smaller than 0.001 m will not improve model performance but cost more simulation time. As such, an increment constant value of 0.001 m should be preferred. CA-ffé was also sensitive to the h_f function parameter. According to the calculated performance indicators, we found that in all test cases, the h_f functions with coefficient a = 0.06 to 0.11 (and b = 0.25) performed better than other functions.

Figure 6 shows sensitivity plots of CA-ffé model parameters using the CSI and NSE performance indicators in Subcatchments 1, 2, and 3 and for Manning's n 0.03, 0.05, and 0.07 $m^{-1/3}s$. In all the three test cases, an increment constant ≤0.001 m produced the best CSI and NSE indicators (see Figures 6a and 6b). The horizontal sensitivity plots in this range showed that in all three subcatchments and for all Manning's n values, the CA-ffé model becomes insensitive to the selected increment constant within this range. This shows that an increment constant of 0.001 m is likely to produce acceptable results in any other case study with a 1-m-grid resolution.

In the case of the h_f function, the accepted performance indicator values in all test cases were produced in the range of a = 0.05 to 0.15 for CSI and a = 0.07 to 0.17 for NSE (see Figures 6c and 6d). Results showed that the accepted range for h_f function slightly changes depending on the surface roughness. In all the test cases with Manning's n = 0.03 $m^{-1/3}s$, the highest performance indicators were achieved when increment constant was smaller than 0.001 m and a was between 0.09 to 0.11. For Manning's n = 0.05 $m^{-1/3}s$, the best performance was achieved when a = 0.1 to 0.13. This range for Manning's n = 0.07 $m^{-1/3}s$ was a = 0.12 to 0.15. This shows

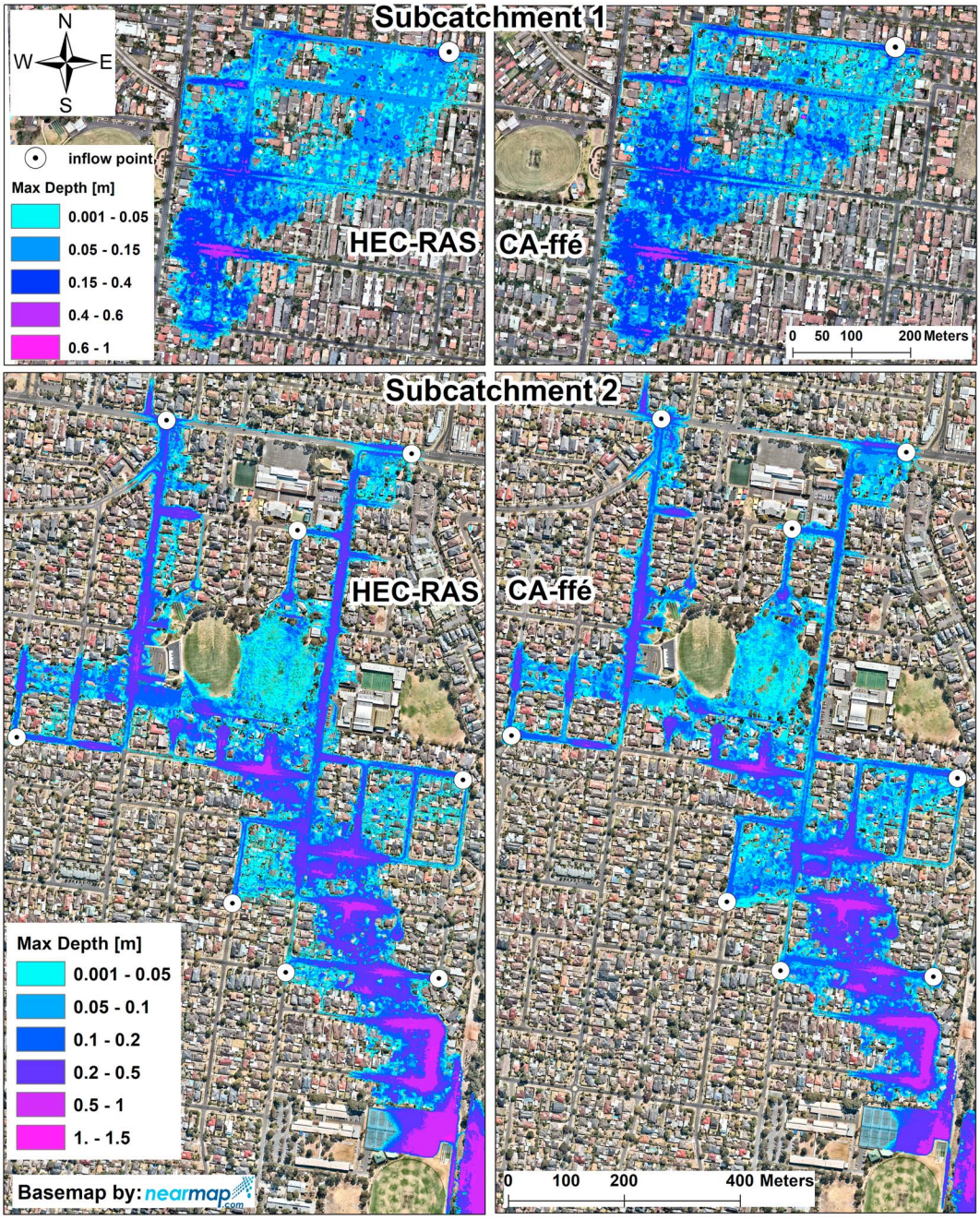

Figure 7. Comparison of the maximum flood depth predicted by HEC-RAS and CA-ffé models in Subcatchments 1 and 2 as well the location of inflow points (for the 100-year event with 1-m-resolution grid). CA-ffé = Cellular Automata fast flood evaluation.

that the coefficient a in the h_f function can describe differences in the surface roughness values. As the surface roughness increased, a larger value of a produced the best performance indicators. The increment constant parameter had the same range among all the test cases. As such, for the rest of the simulations in Subcatchment 4 (Manning's $n = 0.05$ $m^{-1/3}s$) and Test8a (Manning's $n = 0.02$ for roads and 0.05 $m^{-1/3}s$ for other areas) we selected $a = 0.1$ and increment constant of 0.001 m.

3.2. CA-ffé Model Performance

Figures 7 and 8 show the maximum flood extent and depth predicted by CA-ffé and the hydrodynamic models (TUFLOW and HEC-RAS) in Subcatchments 1, 2, 3, and 4. Generally, there was a good

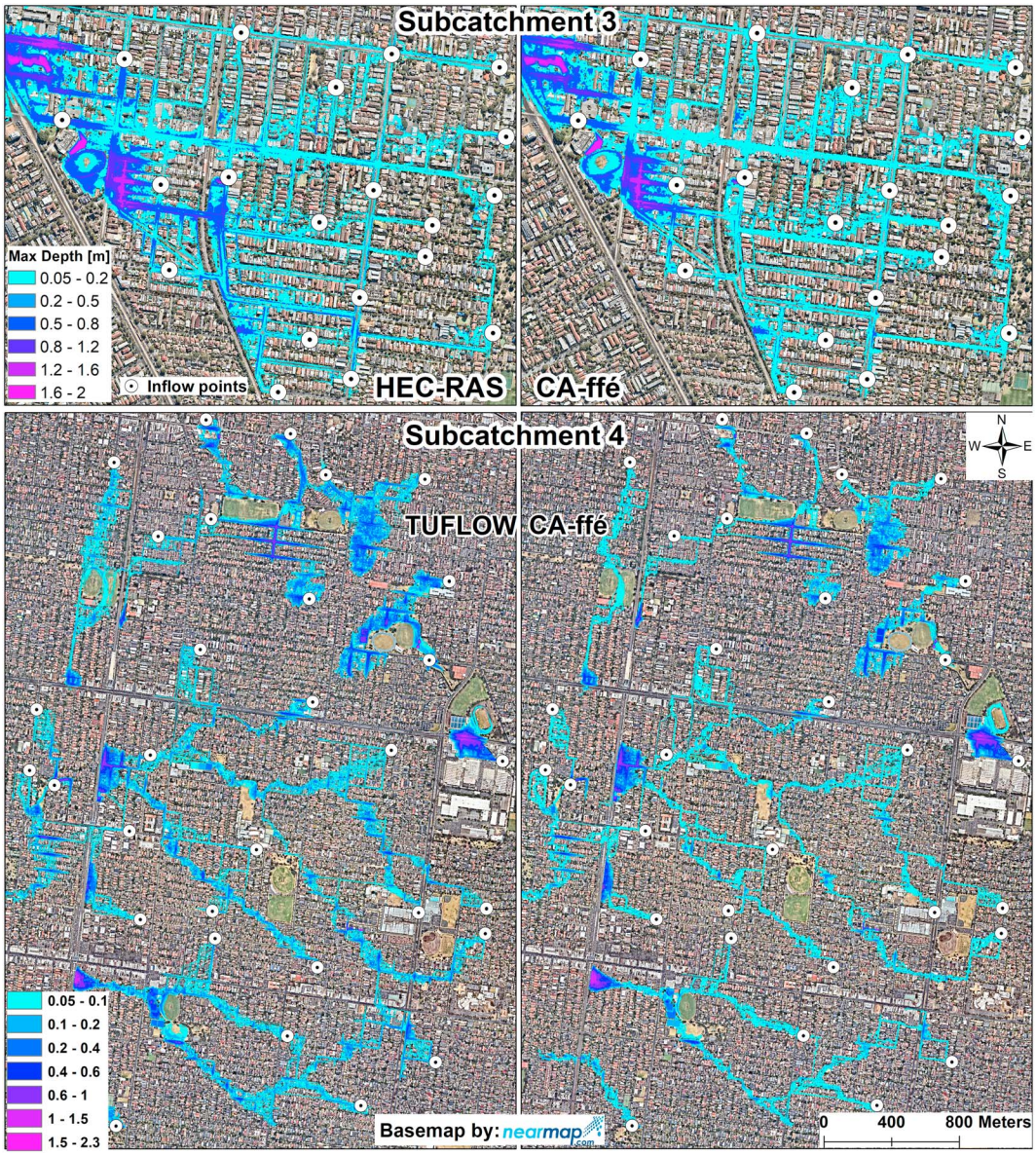

Figure 8. Comparison of maximum flood depth predicted by HEC-RAS and CA-ffé in Subcatchment 3 and predicted by TUFLOW and CA-ffé models in Subcatchment 4 (for the 100-year simulation with 1-m-resolution grid). The location of inflow points is shown with points. CA-ffé = Cellular Automata fast flood evaluation.

agreement between the predicted flood extent by CA-ffé and these models. CA-ffé was able to predict the same inundation extent as the hydrodynamic models in most areas. Figure 9 shows the differences in the predicted water depth by HEC-RAS and CA-ffé models and their frequency distribution. As it can be seen in this figure, the larger difference between the two models usually occurred is in the flow path areas such as streets where water does not pond. On the other hand, in the depression areas, which flood inundation depth is usually significantly higher than flow path areas, CA-ffé's predicted water depth was close to those predicted by HEC-RAS.

Discrepancies between the predicted flood extents were bigger in flow path areas such as streets. This was also observed in Test 8a (Figure 10), where the predicted flood inundation depth and extent in the Centre and the West part of the study area had a better agreement with the TUFLOW and HEC-RAS model results. However, CA-ffé mostly underpredicted flood inundation in the eastern part of the study area where the inflow point was located.

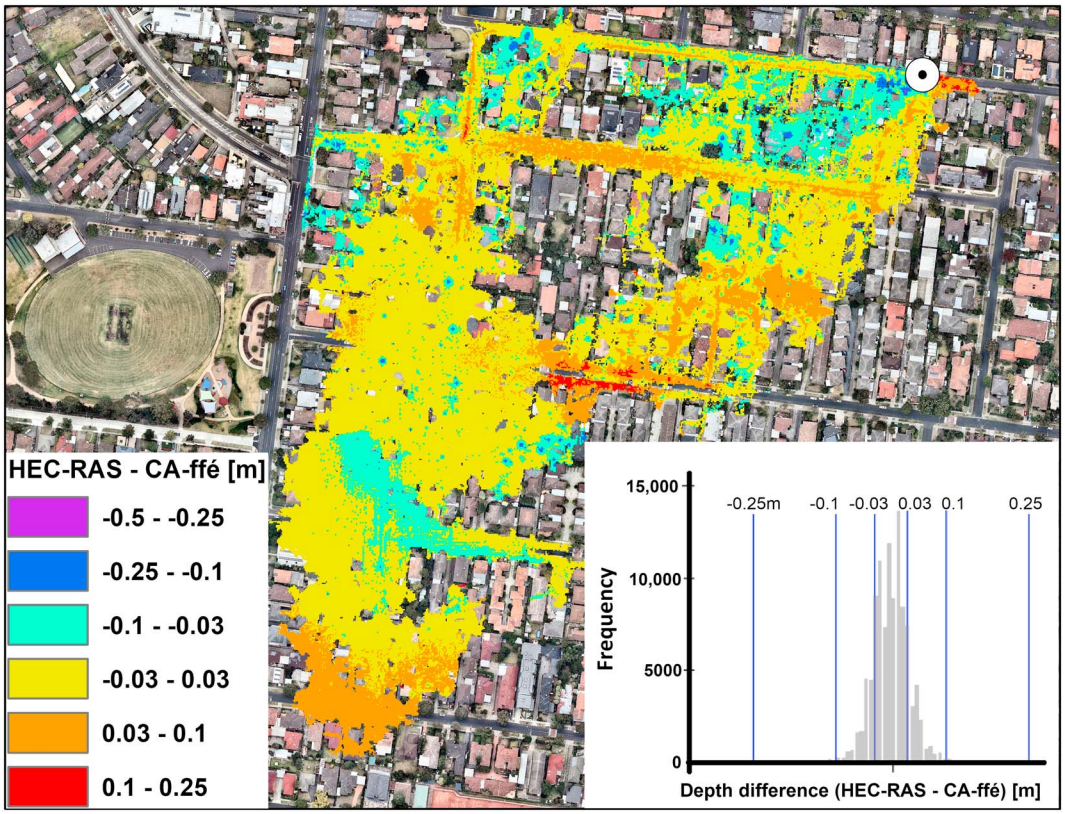

Figure 9. Depth difference between HEC-RAS and CA-ffé in Subcatchment 1 and their frequency distribution. CA-ffé = Cellular Automata fast flood evaluation.

This discrepancy between CA-ffé and the hydrodynamic models' results is most likely due to CA-ffé not representing the flow momentum effects but simply relying on the water balance equation for spreading flood waters. For example, in areas near the inflow point in Test 8a, water depth was dependent on the momentum-related parameters such as flow velocity. In other words, water depth in these areas was more dependent on the shape of the inflow point hydrograph: a higher flow rate would potentially cause higher flood depth in this area. However, the higher inundation depth in the middle of the map was located in a low-lying depression and flooding in this area was mainly dominated by accumulation of water from higher ground and ponding in the depression. Therefore, the flooding in this area was not impacted by the shape of the hydrograph (or hyetograph). A correct prediction of the total flood volume entering this area would lead to a good prediction of water level.

Another explanation for the discrepancy between models in Test 8a was probably the implementation of two different roughness values in the hydrodynamic models (the roughness value for streets and other areas were 0.02 and 0.05 $m^{-1/3}s$, respectively) while the CA-ffé model did not differentiate between land use types. To represent different roughness values (Manning's n) multiple h_f functions can be implemented for each land use type to represent the variability in surface properties. This capability will be added in the future by implementing different h_f functions for each land use type.

Table 3 summarizes the values of the five performance indicators for all the simulation experiments conducted with a grid resolution of 1 m. According to the HR indicator CA-ffé predicted 84% to 95% of cells identified as inundated by the hydrodynamic models. The FAR indicator ranged between 9% and 26%. The CSI range was 70% to 82%. This range for NSE was 0.78 to 0.88. Overall, these indicators show that CA-ffé was able to predict the flood extent and depth produced by the hydrodynamic models with a significant degree of accuracy. Similar performance indicators were achieved when testing CA-ffé for different flood magnitudes in Subcatchment 3. Performance indicators were within the same range among case studies with various surface roughness. No significant difference was observed between the performance of CA-ffé in Test 8a and Subcatchment 4 where we used the calibration results of the first three subcatchments. This indicates

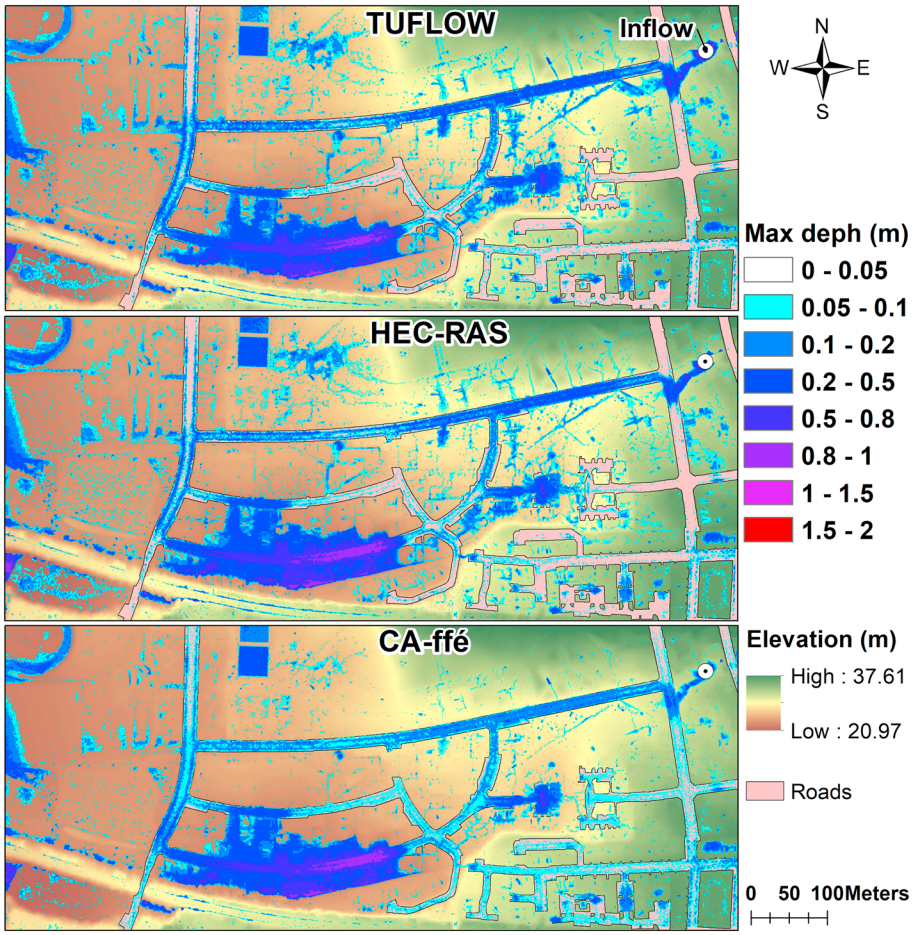

Figure 10. Comparison of maximum flood extents predicted by TUFLOW, HEC-RAS, and CA-ffé models for Test 8a (with 0.5-m-resolution grid). CA-ffé = Cellular Automata fast flood evaluation.

Table 3
Performance Indicator Values Comparing CA-ffé Model Results Against the Hydrodynamic Simulation Models (TUFLOW and HEC-RAS) for 1-m Grid Size

Case study	Validated against	Manning's n ($m^{-1/3}s$)	Total flood volume (1,000 m^3)	Performance indicators				
				HR (%)	FAR (%)	CSI (%)	RMSE (m)	NSE
Subcatchment 1	HEC-RAS	0.03	8 (100-year event)	94.8	16.1	80.2	0.038	0.84
		0.05		91.9	10.6	82.8	0.041	0.81
		0.07		89.9	8.96	82.6	0.046	0.78
Subcatchment 2	HEC-RAS	0.03	24.1 (100-year event)	84.2	14.4	73.7	0.093	0.82
		0.05		85.3	13.1	75.6	0.086	0.81
		0.07		89.6	16.8	75.8	0.079	0.81
Subcatchment 3	HEC-RAS	0.03	50 (100-year event)	86.2	15.9	74.1	0.081	0.88
		0.05		88.2	16.5	75.1	0.084	0.86
		0.07		92.1	20.4	74.8	0.080	0.85
		0.05	28 (50-year)	87.1	14.6	71.3	0.072	0.83
		0.05	10 (10-year)	87.9	14.3	72.2	0.068	0.88
Subcatchment 4	TUFLOW	0.05	111.5 (100-year)	86.8	16.7	74.4	0.064	0.85
Test 8a	TUFLOW	0.02 & 0.05	4.3[a]	88.1	25.2	71.3	0.12	0.83
	HEC-RAS			85.5	26.5	69.3	0.09	0.87

Note. CA-ffé = Cellular Automata fast flood evaluation; HR = hit rate; FAR = false alarm rate; CSI = critical success index; RMSE = root-mean-square error; NSE = and Nash-Sutcliffe efficiency.
[a]This simulation also had 27 mm of rainfall in addition to the point source inflow (see Table 1).

Table 4
Comparison of CA-ffé Model With TUFLOW and HEC-RAS When Different Model Grid Resolutions Applied

	Validated against	Model grid resolution (m)	Performance indicators				
			HR (%)	FAR (%)	CSI (%)	RMSE (m)	NSE
Subcatchment 3[a]	HEC-RAS	1	88.2	16.5	75.1	0.084	0.86
		2	87.5	16.6	73.9	0.087	0.86
		4	84.0	15.9	71.0	0.108	0.81
		5	83.6	12.5	71.8	0.109	0.79
Subcatchment 4	TUFLOW	1	86.8	16.7	74.4	0.064	0.85
		2	89.0	17.9	74.4	0.066	0.83
		4	83.6	18.2	71.6	0.067	0.83
		5	82.8	17.8	71.1	0.068	0.81

Note. CA-ffé = Cellular Automata fast flood evaluation; HR = hit rate; FAR = false alarm rate; CSI = critical success index; RMSE = root-mean-square error; NSE = and Nash-Sutcliffe efficiency.
[a]For the 100-year event with total flood volume of 10,000 m^3 (see Table 1).

that overall, CA-ffé maintained consistency and robustness when applied to different subcatchments and conditions in terms of flood magnitude, surface roughness, catchment size and slope.

3.3. Model Sensitivity to the Grid Size

Table 4 compares the values of performance indicators in Subcatchments 3 and 4 for different model grid resolutions. In general, there is only a slight decrease in model performance with increasing model grid size from 1 to 5 m. In the case of NSE in Subcatchment 3, for example, there was a drop from 0.86 to 0.79 when a 5-m-resolution grid was used. This is most likely because we calibrated CA-ffé with the 1-m-grid resolution and used the same parameters values throughout the rest of the simulations. CA-ffé exhibited consistent performance when tested at different grid resolutions (in the two subcatchments). We therefore conclude that CA-ffé is rather robust even when a 5-m-grid resolution is used.

3.4. Model Computational Performance

Table 5 shows the simulation time for CA-ffé and the hydrodynamic models. Note that when comparing simulation speed of CA-ffé against hydrodynamic models, one should consider that CA-ffé does not predict the same outputs as HEC-RAS and TUFLOW (e.g., flow speed and the spatial-temporal dynamics of flooding). This comparison shows the magnitude of speedup when only the maximum flood inundation is simulated. Nevertheless, CA-ffé simulation times were in the order of a few seconds to 10 min. CA-ffé was 250 to 1,100 times faster than the hydrodynamic models. This simulation time was in the order of the simulation time for the RFM model by Jamali et al. (2018). Generally, the difference between the simulation time of CA-ffé and hydrodynamic models was significant and several order of magnitudes smaller in large or high-resolution case studies. For example, the simulation times of TUFLOW and CA-ffé with a 1-m-grid size in Subcatchment 2 were around 79 hr versus 10 min, respectively, while the 5-m-grid simulation for the same models took 43 min in TUFLOW and 7 s in CA-ffé.

Table 5
Performance indicator values and simulation time of TUFLOW and CA-ffé models

Case study	Validated against	Model grid resolution	Simulation time (h:mm:ss]	
			SWE	CA-ffé
Subcatchment 1	HEC-RAS	1 m	0:40:23	0:00:10
Subcatchment 2	HEC-RAS	1 m	12:45:22	0:00:43
Subcatchment 3	HEC-RAS	1 m	21:32:29	0:02:08
		2 m	2:17:12	0:00:35
		4 m	0:37:45	0:00:07
		5 m	0:18:57	0:00:03
Subcatchment 4	TUFLOW	1 m	79:32:20	0:05:10
		2 m	9:46:16	0:01:33
		4 m	1:20:19	0:00:14
		5 m	0:43:48	0:00:07
Test 8a	TUFLOW	0.5 m	12:24:00	0:03:12
	HEC-RAS	0.5 m	14:35:00	

Note. CA-ffé = Cellular Automata fast flood evaluation; SWE = shallow water equations.

Table 5 shows evidence that CA-ffé is fast and, therefore, has significant potential to be used for flood assessment in different contexts. For example, the model could be used for assessment of flood risk especially in large urban areas. CA-ffé is also suitable for applications in areas that have not yet been mapped for flooding (and for which there may not be resources available to do so, such as in a developing context). It is also suitable for rapidly locating hotspots and problem areas that can later be prioritized for more detailed modeling. Additionally, it could also be used for flood emergency management when we need to either run multiple scenarios for making decisions

about the desired response actions (e.g., we can very quickly test the sensitivities of models and terrain changes like sand bag levees) or, in a real-time context, to update model runs as new data becomes available.

CA-ffé will be further developed to better account for hydrological processes such as infiltration and initial losses when the rainfall on grid method is used. It will also be coupled to the SWMM (Rossman, 2015) to simulate the flooding caused by surcharges from the drainage network and interaction effects with the subsurface network.

4. Conclusions

This paper described the development of a fast flood evaluation model (called CA-ffé) based on the CA approach that only uses topography and water balance equation for spreading floodwater.

We compared CA-ffé against two widely used hydrodynamic models (TUFLOW and HEC-RAS) by simulating the maximum flood inundation extent and depth caused by storm sewer surcharges and direct rainfall in four different urban subcatchments. CA-ffé was able to simulate most of the flow paths and inundated areas predicted by TUFLOW and HEC-RAS, with some discrepancies. CA-ffé performs well in predicting the inundation depth and extent in low-lying depression areas (which usually have higher inundation depths and are potentially associated with greater risk and damage). However, in areas where flood water has higher momentum and velocity, CA-ffé was not able to predict inundation depths with the same accuracy.

Our analyses showed that CA-ffé's performance is dependent on the selected model parameters (the h_f function and increment constant value) but not significantly impacted by increasing the grid size from 1 to 5 m. The range of model parameters for which the best performance indicators were achieved was consistent in different case studies and conditions (e.g., various catchment characteristics, flood magnitudes, surface roughness, and model grid resolution). Using the best parameter range from the sensitivity analysis produced similar performance in other case studies. Therefore, it could be concluded that CA ffé is a robust model that performs consistently in different flood conditions. We concluded that the model is rather robust even when a 5-m-grid resolution is used, which is beneficial for applications in areas where data limitations are apparent. When no detailed hydrodynamic model result is available for calibrating the model parameters, CA-ffé should be used with the suggested parameter from this study.

CA-ffé model is easy to set up and implement. Most importantly, it was able to simulate a typical flood event within seconds to 10 min (depending on the size of and terrain resolution of the catchment). This makes CA-ffé suitable for applications that require many simulations, not require velocity output, and have low demands on the representation and accuracy of flow dynamics.

Acknowledgments
Behzad Jamali acknowledges the support from Monash University in the form of a Monash Graduate Scholarship (MGS) and Monash International Postgraduate Research Scholarship (MIPRS). This study is also supported by the Australia-Indonesia Centre (AIC) under the project code RCC-BrownMON: Urban Water Cluster and fund code SRP16 52057764. The authors would like to thank João Paulo Leitão, Roland Löwe, and Karsten Arnbjerg-Nielsen for their inputs to this research. Digital elevation model (DEM) for the Melbourne case studies was from the Bayside LiDAR Project. We also would like to thank the two anonymous reviewers and Associate Editor for their suggestions and comments. DEM and drainage network data for Melbourne case studies were kindly provided by Melbourne Water (www.melbournewater.com.au/). Readers can download these data from the website (https://data.mendeley.com/datasets/jfvwgrgrth/draft?a=9cf6382f-4d2e-493e-8fe8-21589690eae5). The input data for the Test 8A case study were from Néelz and Pender (2013).

References

Apel, H., Martínez Trepat, O., Hung, N. N., Chinh, D. T., Merz, B., & Dung, N. V. (2016). Combined fluvial and pluvial urban flood hazard analysis: Concept development and application to Can Tho city, Mekong Delta, Vietnam. *Natural Hazards and Earth System Sciences*, *16*(4), 941–961. https://doi.org/10.5194/nhess-16-941-2016

Bates, P. D., & de Roo, A. P. J. (2000). A simple raster-based model for flood inundation simulation. *Journal of Hydrology*, *236*(1-2), 54–77. https://doi.org/10.1016/S0022-1694(00)00278-X

Bates, P. D., Horritt, M. S., & Fewtrell, T. J. (2010). A simple inertial formulation of the shallow water equations for efficient two-dimensional flood inundation modelling. *Journal of Hydrology*, *387*(1-2), 33–45. https://doi.org/10.1016/j.jhydrol.2010.03.027

Bennett, N. D., Croke, B. F. W., Guariso, G., Guillaume, J. H. A., Hamilton, S. H., Jakeman, A. J., et al. (2013). Characterising performance of environmental models. *Environmental Modelling & Software*, *40*, 1–20. https://doi.org/10.1016/j.envsoft.2012.09.011

Bernini, A., & Franchini, M. (2013). A rapid model for delimiting flooded areas. *Water Resources Management*, *27*, 3825–3846. https://doi.org/10.1007/s11269-013-0383-3

CH2M (2013). ISIS FAST. Retrieved from http://help.floodmodeller.com/isis/ISIS_Fast.htm

Chen, A. S., Djordjevic, S., Leandro, J., & Savic, D. (2007). The urban inundation model with bidirectional flow interaction between 2D overland surface and 1D sewer networks. NOVATECH 2007.

Chen, A. S., Evans, B., Djordjević, S., & Savić, D. A. (2012). Multi-layered coarse grid modelling in 2D urban flood simulations. *Journal of Hydrology*, *470*, 1–11. https://doi.org/10.1016/j.jhydrol.2012.06.022

de Sousa, L. M., Gibson, M., Chen, A. S., Savic, D., & Leitão, J. P. (2017). Exploring the advantages of hexagonal raster for flood modelling using cellular automata. Paper presented at the 14th IWA/IAHR International Conference on Urban Drainage ICUD, Prague.

Dottori, F., & Todini, E. (2011). Developments of a flood inundation model based on the cellular automata approach: Testing different methods to improve model performance. *Physics and Chemistry of the Earth, Parts A/B/C*, *36*(7-8), 266–280. https://doi.org/10.1016/j.pce.2011.02.004

EA (2012). Two dimensional modelling in urban and rural floodplains. Retrieved from Australia:

ESRI (2012). ArcGIS desktop: Release 10. In E. S. R. Institute (Ed.).

GDAL Development Team (2018). GDAL—Geospatial Data Abstraction Library, Version 2.2.3: Open Source Geospatial Foundation. Retrieved from http://www.gdal.org

Ghimire, B., Chen, A. S., Guidolin, M., Keedwell, E. C., Djordjević, S., & Savić, D. A. (2013). Formulation of a fast 2D urban pluvial flood model using a cellular automata approach. *Journal of Hydroinformatics*, *15*(3), 676–686. https://doi.org/10.2166/hydro.2012.245

Gouldby, B., Sayers, P., Mulet-Marti, J., Hassan, M. A. A. M., & Benwell, D. (2008). A methodology for regional-scale flood risk assessment. *Proceedings of the Institution of Civil Engineers: Water Management*, *161*(3), 169–182. https://doi.org/10.1680/wama.2008.161.3.169

Guidolin, M., Chen, A. S., Ghimire, B., Keedwell, E. C., Djordjević, S., & Savić, D. A. (2016). A weighted cellular automata 2D inundation model for rapid flood analysis. *Environmental Modelling & Software*, *84*, 378–394. https://doi.org/10.1016/j.envsoft.2016.07.008

Hydrologic Engineering Center (2016). HEC-RAS River Analysis System. 2D modeling user's manual. Version 5.0.

Innovyze (2012). InfoWorks ICM Help v3.0. Retrieved from.

Jamali, B., Löwe, R., Bach, P. M., Urich, C., Arnbjerg-Nielsen, K., & Deletic, A. (2018). A rapid urban flood inundation and damage assessment model. *Journal of Hydrology*, *564*, 1085–1098. https://doi.org/10.1016/j.jhydrol.2018.07.064

Kaspersen, P. S., & Halsnæs, K. (2017). Integrated climate change risk assessment: A practical application for urban flooding during extreme precipitation. *Climate Services*, *6*, 55–64. https://doi.org/10.1016/j.cliser.2017.06.012

Krupka, M. (2009). *A Rapid Inundation Flood Cell Model for Flood Risk Analysis*. Edinburgh, Scotland: Heriot-Watt University.

Lhomme, J., Sayers, P., Gouldby, B., Samuels, P., Wills, M., & Mulet-Marti, J. (2008). Recent development and application of a rapid flood spreading method. https://doi.org/10.1201/9780203883020.ch2.

Liu, Y., & Pender, G. (2010). A new rapid flood inundation model. Paper presented at the proceedings of the first IAHR European Congress.

Löwe, R., Urich, C., Sto. Domingo, N., Mark, O., Deletic, A., & Arnbjerg-Nielsen, K. (2017). Assessment of urban pluvial flood risk and efficiency of adaptation options through simulations—A new generation of urban planning tools. *Journal of Hydrology*, *550*, 355–367. https://doi.org/10.1016/j.jhydrol.2017.05.009

Néelz, S. (2009). Desktop review of 2D hydraulic modelling packages (1849110794). Retrieved from.

Néelz, S., & Pender, G. (2013). Benchmarking the latest generation of 2D hydraulic modelling packages (SC120002). Retrieved from Environment Agency.

Rossman, L. A. (2015). Storm water management model user's manual version 5.1 (EPA/600/R-14/413). Retrieved from Washington, DC: http://nepis.epa.gov/Exe/ZyPDF.cgi?Dockey=P100N3J6.TXT.

Sampson, C. C., Smith, A. M., Bates, P. D., Neal, J. C., Alfieri, L., & Freer, J. E. (2015). A high-resolution global flood hazard model. *Water Resources Research*, *51*, 7358–7381. https://doi.org/10.1002/2015WR016954

Shao, Q., Weatherley, D., Huang, L., & Baumgartl, T. (2015). RunCA: A cellular automata model for simulating surface runoff at different scales. *Journal of Hydrology*, *529*, 816–829. https://doi.org/10.1016/j.jhydrol.2015.09.003

Simões, N., Ochoa-Rodríguez, S., Wang, L.-P., Pina, R., Marques, A., Onof, C., & Leitão, J. (2015). Stochastic urban pluvial flood hazard maps based upon a spatial-temporal rainfall generator. *Water*, *7*(12), 3396–3406. https://doi.org/10.3390/w7073396

Teng, J., Jakeman, A. J., Vaze, J., Croke, B. F. W., Dutta, D., & Kim, S. (2017). Flood inundation modelling: A review of methods, recent advances and uncertainty analysis. *Environmental Modelling & Software*, *90*, 201–216. https://doi.org/10.1016/j.envsoft.2017.01.006

WBM, B. (2016). TUFLOW User Manual – Build 2016-03-AA. In.

Wing, O. E. J., Bates, P. D., Sampson, C. C., Smith, A. M., Johnson, K. A., & Erickson, T. A. (2017). Validation of a 30 m resolution flood hazard model of the conterminous United States. *Water Resources Research*, *53*, 7968–7986. https://doi.org/10.1002/2017wr020917